Microelectronic Engineering xxx (xxxx) xxx

Contents lists available at ScienceDirect

Microelectronic Engineering

journal homepage: www.elsevier.com/locate/mee

Research paper

Simple method for determining Si p-n junction depth using anodization

E. Hourdakis [a,*], G. Pepponi [b], M. Barozzi [b], A.G. Nassiopoulou [a]

[a] NCSR Demokritos, Institute of Nanoscience and Nanotechnology (INN), Patriarchou Grigoriou & Neapoleos 27, Aghia Paraskevi, 153 10 Athens, Greece
[b] FBK, CMM, Micro Nano Facility, via Sommarive, 18, 38123 Trento, Italy

ARTICLE INFO

Keywords:
Si p+/n junction
Porous Si
Junction depth determination

ABSTRACT

A simple method for the determination of a Si p+/n junction depth is presented. The method is designed to delineate the specific junction due to its importance in the field of Si solar cells where cost effective and fast characterization techniques are necessary. It consists of the electrochemical transformation of the p+ Si to porous Si. The determination of the porous Si depth with the use of cross-sectional Scanning Electron Microscope (SEM) images provides a direct, fast and easy to implement measurement of the junction depth. In addition, through a simple 4-point probe electrical measurement of the sheet resistance, the average dopant concentration is determined, which allows the creation of an abrupt junction approximation of the p+/n junction. The method is shown to produce accurate results in two types of doping techniques, namely implantation and spin-on-doping and a range of junction depths between 200 nm and 1500 nm, as compared to the well-established secondary ion mass spectrometry (SIMS) technique.

1. Introduction

The determination of p-n junction characteristics, such as the junction depth and dopant profile, is necessary both in microelectronics and solar cell applications. To that end, a number of well-established techniques are commonly used in the field, with the most notable being the spreading resistance (SR) and the differential Hall (DH) in terms of electrical characterization and secondary ion mass spectrometry (SIMS) and sputtered neutral mass spectrometry (SNMS) in terms of atomic dopant distribution characterization. All of the mentioned techniques suffer from disadvantages that stem from the complexity of their implementation, a fact detrimental to their use in applications such as the solar cells, where speed and simplicity often outweigh the need for accuracy. For example, SR and DH can be very tedious and time consuming, while SIMS and SNMS require expensive instrumentation. For those reasons, simple and fast techniques for the delineation of p-n junctions are constantly being researched.

Two such methods that have been presented in the literature that involve simple electrochemical processes are a) the electrochemical capacitance-voltage profiling and b) the profiling using the formation of porous Si through anodization. In the first category, the capacitance vs. voltage measurement of the Schottky barrier created between the Si sample and an electrolyte at one or more frequencies provides information on the doping concentration at the very surface of the Si sample [1–5]. Once the information is extracted, electrochemical dissolution of the Si is performed and the process is repeated, until the doping profile is determined. The iterations required to reach the junction depth can be many and so this method can be rather time consuming. In addition, the choice of the appropriate frequencies for the measurements can be a source of further complication. Finally, this method requires large areas so that the capacitance caused by the edges of the etched pits does not significantly contribute to the total measured capacitance.

On the other hand, the electrochemical creation of porous Si through anodization has been demonstrated to provide a rather good dopant profiling in a very simple manner [6–8]. It has been shown that the anodization potential (the voltage across the electrolyte/Si barrier), for a constant applied current, depends on the surface dopant concentration through the relation [6]:

$$V = C' - \frac{1}{C_H}\sqrt{2q\varepsilon_S\left(\psi_S - \frac{kT}{q}\right)N_A}$$

where C′ is a constant, C_H is the Helmholtz capacitance and ψ_S is the potential barrier at the electrolyte/Si interface, k is the Boltzmann constant, q is the electronic charge, ε_S is the dielectric constant, T is the

* Corresponding author.
E-mail addresses: m.hourdakis@inn.demokritos.gr (E. Hourdakis), pepponi@fbk.eu (G. Pepponi), barozzi@fbk.eu (M. Barozzi), A.Nassiopoulou@inn.demokritos.gr (A.G. Nassiopoulou).

https://doi.org/10.1016/j.mee.2021.111558
Received 8 March 2021;
Available online 4 May 2021

Table 1
Fabrication conditions for all samples used in this work.

Sample name	Doping method	Implantation energy (keV)	Annealing atmosphere	Annealing temperature (°C)	Annealing time (min)
IMP_1a	Implantation	60	N_2	1050	30
IMP_1b	Implantation	150	N_2	1050	30
SOD_1a	Spin-on dopant	–	75% N_2/25% O_2	1050	120
SOD_1b	Spin-on dopant	–	75% N_2/25% O_2	900	30

temperature and N_A is the acceptor concentration at that interface. A calibration curve of the anodization potential of a sample of known doping profile is used to determine the values of the constants involved. This method is very simple both in its application and in the interpretation of its results. It is limited by the fact that porous Si can only be created on p-type Si (under no illumination) [9]. So far, the only references on this interesting method that the authors are aware have examined p-type Si implanted with boron creating p+/p-type samples. In such samples the anodization continues indefinitely with time and so the anodization potential needs only to be monitored against the elapsed time which, in turn, can be correlated to the porous Si depth.

In this work, a simple method for extracting p-n junction characteristics based on the electrochemical creation of porous Si is presented. In contrast to the previously mentioned technique, the method is designed to determine the junction depth, as well as an abrupt junction approximation of p+/n junctions due to their importance in the crystalline Si solar cell application. In this field, the n-type substrate has gained increasing interest due to its demonstrated relative tolerance to common impurities like iron and oxygen and its immunity to boron-oxygen light-induced degradation which is reported in p-type crystalline Si solar cells [10,11]. For n-type substrate solar cells a highly doped (p+) layer on n-Si is used as the collector [12–14]. A fast and easy to implement method for the determination of the basic characteristics of this collector is thus very important. In the presented method, a single anodization step transforms the entire p+ region of the Si substrate to porous Si in a self-limited manner, since the n-type Si substrate constitutes an etch stop for this process [9]. SEM imaging of the porous Si depth then allows the determination of the p+/n junction depth in a very straightforward process. A similar idea has been presented in a patent [15], but the authors of the current work have not been able to find a relevant publication on the subject. In addition, the determination of the junction depth is also combined with a simple 4-point probe measurement of the sheet resistance in this work which allows the creation of an abrupt junction approximation, as an expansion of the central idea. The demonstration of the use of porous Si creation for the determination of the junction depth, its theoretical analysis and the creation of the abrupt junction approximation constitutes the novel method presented. Even though the presented method does not provide a dopant depth profile, we believe it provides significant information on a technologically important type of p-n junction in a very simple, fast manner that requires no expensive instrumentation and almost no data analysis.

2. Sample preparation

Two different types of samples were fabricated, both containing a p+/n junction on n-type Si. The resistivity of the Si substrate was (1-2Ωcm). In the first type the junction was formed by boron ion implantation, while in the second type the technique of spin-on-doping (SOD) was used. The two different techniques were used to create junctions with a large variety of depths and to demonstrate the generality of the proposed method.

In the case of ion implantation a BF_2 ion source was used. Ion implantation was performed at two different energies, namely 60 keV (sample IMP_1a) and 150 keV (sample IMP_1b). For both samples the dose used was 10^{16} ions/cm^2 and annealing was performed at 1050 °C for 30 min in an N_2 ambient.

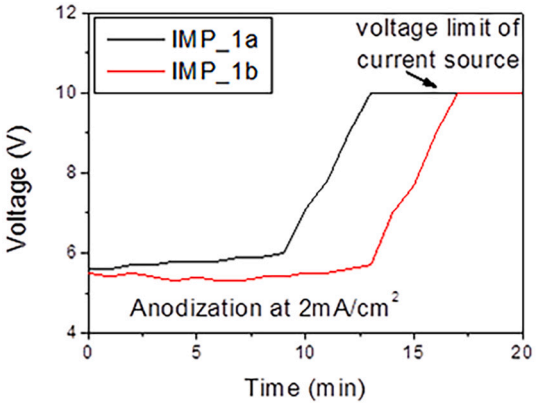

Fig. 1. Voltage during anodization as a function of time for the two implanted samples. The voltage remains almost constant until the p-n junction is reached. It then increases rapidly up to the voltage limit of the current source. The process is therefore self-limited.

With the SOD process two different samples were fabricated, namely samples SOD_1a and SOD_1b. The SOD material was B154 from Filmtronics (3.8% Boron). Spinning was performed on 3-in. Si wafers at 3000 rpm for 30s. After spinning, the film was hard baked at 200 °C for 15 min on a hot plate. The wafer was then cut in 2 pieces and two different annealing conditions were used. The atmosphere in both cases was 75% N_2 and 25% O_2. Sample SOD_1a was annealed at 1050 °C for 120 min and SOD_1b at 900 °C for 30 min. After annealing the SOD film was removed by dipping the sample in buffered HF (BHF, 7:1 HF (50% in H_2O):NH_4F) for 15 min. The fabrication conditions for all samples are presented in Table 1.

3. Method for junction delineation

As described in the introduction, our method used for junction delineation is based on the fact that we can selectively electrochemically transform p- or p+-type Si to porous Si through anodization without affecting the n-type substrate, which constitutes an etch stop for the specific process. We anodized all of our samples until the etch stop, thus transforming the entire p+ layer into porous Si. Anodization was performed in an HF:ethanol solution with 60:40 volume ratio and constant current density of 2 mA/cm^2. The value of the current density used for the anodization was chosen to be the lowest possible for our electrolyte composition. During the anodization, the sample is the anode, while a platinum electrode in the electrolyte acts as the cathode. With this configuration a forward biased Schottky barrier is created between the sample top surface and the electrolyte. On the other hand, the p-n junction is reverse biased. So, the larger the current value used, the larger the depletion width of this junction would be. So, in order to probe the correct junction depth, this depletion width should be minimized by minimizing the current value.

The end of anodization was determined by monitoring the anodization voltage. At the junction depth this voltage started to rapidly increase up to the voltage limit of the current source set at 10 V for all experiments. The process is therefore self-limited. Voltage vs. time curves of the anodization process are presented in Fig. 1 for both

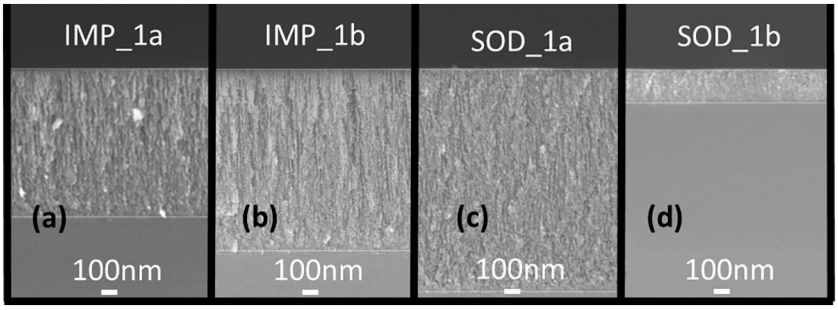

Fig. 2. Cross sectional SEM images of sample (a) IMP_1a, (b) IMP_1b, (c) SOD_1a and (d) SOD_1b. The porous Si layer is clearly visible on the top side of the Si substrate, in all cases.

Table 2
Porous Si depth, sheet resistance and average doping density for all samples.

Sample name	Porous Si depth (nm)	Sheet resistance (Ω/square)	Average boron concentration from sheet resistance (at/cm^3)
IMP_1a	926	23.2	5.3×10^{19}
IMP_1b	1158	17.6	5.6×10^{19}
SOD_1a	1500	40.4	1.6×10^{19}
SOD_1b	220	264.0	1.8×10^{19}

implanted samples. These results are representative of all samples. Usually, the voltage during anodization for these conditions is of the order of a few hundred millivolts. In this case, though, large potential drops caused by the reverse biased p-n junction and the contact resistance of the back side of the samples during anodization are added to the total voltage of the system. No effort to create an Ohmic back contact to the samples was made, in order not to increase the complexity of the method.

The depth of the produced porous Si layer is a direct measure of the junction depth. In order to measure the porous Si depth, the samples were cut and cross sectional Scanning Electron Microscope (SEM) images were obtained. These are presented in Fig. 2 for all samples. Using these, the depth of the porous Si layer was determined. The results are presented in Table 2.

We also used electrical characterization of our samples. The four point probe method was used and the sheet resistance $\rho_S = \rho/t = 4.532$ V/I of all samples, before anodization, was obtained and is presented in Table 2. Using this measurement and the porous Si depth (t in the last equation), the average resistivity and, in turn, the average boron concentration of the boron doped part of the junction was deduced. This is also presented in Table 2 for all samples.

Using the results of our novel method, namely the porous Si depth (junction depth) and the sheet resistance (average boron concentration) we create an abrupt junction approximation of the p-n junction under consideration in a very simple, fast and easy to implement manner. It is worth noting that our proposed method produces approximations for junctions that span a wide range of depths.

4. Discussion

In order to confirm the validity of our method the obtained results described above were compared with a well-established method for depth profiling, namely secondary ion mass spectrometry (SIMS). SIMS is performed by sputtering the sample with a primary ion beam, while measuring at each depth the secondary ion intensity of the specific element by mass spectrometry. The secondary ion intensity is then converted into an atomic concentration by using the relative sensitivity factor RSF obtained on a reference sample with known dopant concentration. In our case, boron concentration as a function of depth was registered. An example of this, namely the measurements for sample IMP_1a are presented in Fig. 3. Fig. 3(a) presents the SIMS results in a logarithmic scale, while Fig. 3(b) in a linear scale. In addition to the SIMS results, the results of our method are also presented in these graphs for comparison, along with a linear fit of the SIMS results. From Fig. 3 it is evident that sample IMP_1a consists of a junction that after the first few hundreds of nanometers becomes linearly graded. This is the case for all samples presented here, as will be shown later.

It becomes evident that the porous Si depth is very close to the end of the linearly graded region of the junction. Below this point a slower decrease in boron concentration down to the noise floor of the measurement exists. This “tail” in the SIMS measurements is a common

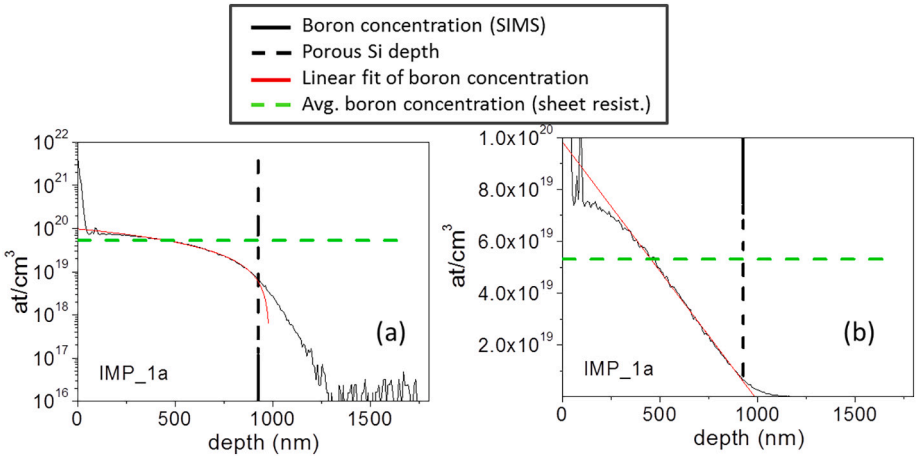

Fig. 3. Boron concentration as a function of depth for sample IMP_1a in (a) logarithmic and (b) linear scale. Porous Si depth and average boron concentration measured by our novel method are also presented in the figures along with a linear fit for the linearly graded part of junction.

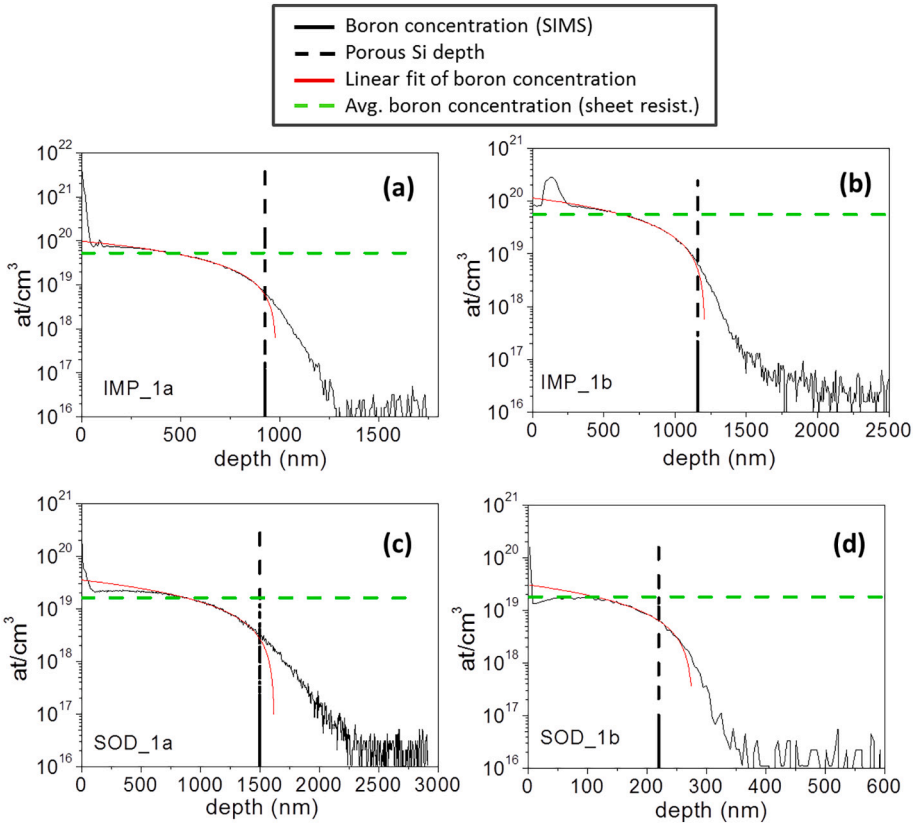

Fig. 4. Boron concentration as a function of depth for sample (a) IMP_1a, (b) IMP_1b, (c) SOD_1a and (d) SOD_1b in logarithmic scale. Porous Si depth and average boron concentration measured by our novel method are also presented in the figures along with a linear fit for the linearly graded part of junction.

source of discrepancy between this technique and electrical profiling techniques that measure carrier profiles [16,17]. Its origin may be the existence of cascade mixing and knock-on of dopant atoms by the sputtering beam. The turning point between p-type and n-type Si should be the point at which the boron dopants become less than the phosphorus dopants of the substrate. Considering the resistivity of the n-type substrate (1-2Ωcm) this should be when the boron dopant concentration becomes less than 10^{16}at/cm^3, the detection limit of the SIMS measurements. Perhaps a better measure of the actual junction (electrically) can be found in assuming a linearly graded junction on the p-type side with a constant n-type concentration. We can use the linear fit of the linearly graded part of the junction to calculate the intersection with the 10^{16}at/cm^3 concentration point. That point is at a depth of 974 nm, which is very close to the value indicated by the porous Si depth measurement which, as was shown earlier, is 926 nm. The difference between the two values is 48 nm, or almost 5%. Experimental errors in this case include mainly the SEM measurement accuracy and the calibration of the depth scale of SIMS. For the latter, SIMS results were calibrated against samples of known concentrations, as was discussed earlier. For the SEM measurements, several measurements on the same sample were performed leading to an average of the quoted value of 926 nm with a maximum relative error of 10 nm. We therefore believe that the discrepancy between the two values cannot be explained by measurement errors, which we do not think exceed a ± 20 nm, taking into account SEM and SIMS errors. In contrast, we believe that the porous Si depth is smaller due to the existence of a depletion layer near the metallurgical junction which is enhanced during anodization due to the reverse-biased junction [18].

In fact, we can estimate the value of this depletion width (W) assuming a linearly graded junction close to the metallurgical junction by using the linear slope (α) extracted from the SIMS results. Then we have [18]:

$$W = \left(\frac{12\varepsilon_0\varepsilon_{Si}(\psi_{bi} - V)}{qa}\right)^{1/3}$$

where ε_0 is the permittivity of vacuum, ε_{Si} is the dielectric constant of Si, ψ_{bi} is the junction's built-in potential, V is the applied potential across the junction and q is the charge of the electron. In the case of the results presented in Fig. 3, the value of a is 1.04×10^{24}(at/cm^4). From ref. [18] we determine that for this value of slope, ψ_{bi} is close to 0.9 V and so, since the junction is reversed biased during anodization with a minimal amount of current we will assume that ψ_{bi}-V is close to 1 V. With these assumptions we calculate a depletion width of 42 nm, a value very close to the difference between the porous Si depth and the interception of the linear fit of the SIMS results and the 10^{16}at/cm^3 point which is 48 nm and now well within the experimental error estimations for our measurements.

In order to better demonstrate the effect that this depletion width has on the measured porous Si depth we have performed anodization of samples identical to sample IMP_1a under larger current densities, namely 10 mA/cm^2 and 20 mA/cm^2. These values push the junction into more reverse biased conditions thereby increasing the depletion width and therefore reducing the produced porous Si depth. In fact, the porous Si depth, for these current densities, is measured to be 867 and 790 nm respectively. Since the SIMS results remain the same in all cases and the experimental errors of the SEM measurements are unaffected by the current densities, we believe that these results demonstrate the role of the depletion width in the produced porous Si thicknesses. They also provide motivation for the use of the smallest possible current density, namely 2 mA/cm^2, for the results presented herein. Moreover, it becomes obvious that the more abrupt the created junction, the better our method would work. The depletion width within the p-side of the junction exists only because of the linearity of the boron concentration close to the actual junction. For a theoretically abrupt p+/n junction no

Table 3
Linear region slope from the SIMS measurements, linear interception with the 10^{16}at/cm^3 concentration point, porous Si depth and the difference between the latter two for all samples. Also presented are the estimate of the depletion width in each case as well as the sheet resistance calculated form the SIMS results and the measured sheet resistance.

Sample	Linear region slope from SIMS (at/cm^4)	Linear region interception with 10^{16}at/cm^3 (nm)	Porous Si depth (nm)	Difference between linear interception and porous Si depth (nm)	Depletion width (nm)	Sheet resistance (from SIMS) (Ω/square)	Sheet resistance (measurement) (Ω/square)
IMP_1a	1.04×10^{24}	974	926	48	42	19.1	23.2
IMP_1b	9.74×10^{23}	1201	1158	43	43	14.7	17.6
SOD_1a	2.21×10^{23}	1620	1500	120	71	35.5	40.4
SOD_1b	1.13×10^{24}	276	220	56	41	251.8	264

Table 4
Number of boron atoms/cm^2 (SIMS) and number of holes/cm^2 (our method) for the junctions in all samples.

Sample	Boron atoms/cm^2 (SIMS)	Holes/cm^2 (our method)
IMP_1a	5.2×10^{15}	4.9×10^{15}
IMP_1b	8.4×10^{15}	6.5×10^{15}
SOD_1a	2.7×10^{15}	2.4×10^{15}
SOD_1b	3.9×10^{14}	3.6×10^{14}

depletion would exist in the p+ side. This would mean that the porous Si depth would be exactly the same as the junction depth. For this reason, we believe, that our method would work very well even for shallow p+/n junctions which are of the most relevance technologically.

The results presented for sample IMP_1a are characteristic for all samples. In Fig. 4, boron concentration as a function of depth from the SIMS measurements are presented for all samples in a logarithmic scale. The results of our method, namely porous Si depth and average boron concentration from the sheet resistance measurements, and the linear fit of the linearly graded part of the junctions are also presented. The results of the analysis described above for sample IMP_1a is presented in Table 3 for all samples. We note that the linear interception with the 10^{16}at/cm^3 point is very close to the porous Si depth for all samples, albeit a little higher due to the presence of a depletion layer. An estimate of the depletion width expected in each case, based on the analysis presented above, is also given for all samples in Table 3. We believe that these results constitute evidence that the porous Si depth is a good measure of the true electrical junction depth, validating this part of our proposed method.

The SIMS results have also been used to calculate the expected sheet resistance of our samples, assuming that the boron concentration is the same as the hole concentration for our samples. This assumption is certainly not entirely correct, but it allows the estimation of the sheet resistance. So, it is [17]:

$$\rho_S = \frac{1}{q\int_0^t [n(x)\mu_n(x) + p(x)\mu_p(x)]dx} \approx \frac{1}{q\int_0^t [p(x)\mu_p(x)]dx}$$

where q is the charge of the electron, t is the junction depth, n is the electron and p is the hole concentrations at any given depth x and μ is the mobility of the respective carriers. In our case, the hole concentration dominates over the junction depth. The mobility also depends on the carrier density through the relation [[17] appendix 8.1]:

$$\mu_p = \mu_0 e^{-p_c/p} + \frac{\mu_{max}}{\left[1 + \left(p/C_r\right)^a\right]} - \frac{\mu_1}{\left[1 + \left(C_S/p\right)^b\right]}$$

The definitions and values of the various constants can be found in [[17] appendix 8.1]. The calculated sheet resistance values are presented in Table 3 along with the measured values for all samples. It can be seen that the measured values are very close to the calculated ones even though slightly larger. We believe that this is mostly the result of the assumption that the boron concentration is equal to the hole concentration, in other words that the boron is completely activated.

Having validated the two measurements of our proposed method (junction depth and sheet resistance) through the use of the SIMS technique, we compare the abrupt junction approximation to the SIMS results by comparing the integral of the two. Mathematically this is respectively the area under the SIMS depth profile for the boron concentration and the abrupt junction approximation curves. Physically it is the number of boron atoms under a 1cm^2 area for the SIMS case, while it is the number of holes under a 1 cm^2 area for the case of our abrupt junction approximation. These results are presented in Table 4. Ideally, the value of the SIMS integral should equal the implantation dose for samples IMP_1a and IMP_1b. In our case, though, the post-implantation annealing was performed without a screening oxide and so the lower numbers reflect the out-diffusion of boron atoms during that process. From the results presented in Table 4 it can be seen that our method provides a rather good approximation of the junction. Considering the limitations discussed in the junction depth (namely the existence of a small depletion layer in the p-type side during anodization) and the electrical results (the assumption that all boron atoms are activated), the integrals presented in Fig. 4 are very close. Moreover, the larger deviations exist in the cases where the SIMS results reveal large peaks near the surface of the samples (IMP_1b) which may very well be high concentrations of non-activated boron atoms.

5. Conclusions

In conclusion, we present a method for providing an abrupt junction approximation of a p+/n junction. The method consists of anodizing the p+ part of the junction and, by measuring the porous Si depth, providing a direct measurement of the junction depth. In addition, a sheet resistance measurement provides a value of the average dopant concentration of the junction down to its depth. The method is validated against a well-established technique for depth profiling, namely SIMS, and was shown to produce good quality results for two doping techniques (implantation and Spin-On-Doping) and for a wide range of junction depths (from 220 nm to 1500 nm). We also show the applicability of our method for even smaller junction depths. The proposed method is fast, easy to implement and does not require expensive instrumentation, calibration samples, complicated processing or analysis for its implementation. It is thus very interesting for applications where cost and speed outweigh the precision of the analysis, such as the p+/n junction solar cells.

Declaration of Competing Interest

The authors declare that they have no known competing financial interests or personal relationships that could have appeared to influence the work reported in this paper.

Acknowledgements

This work has received funding from the Hellenic Foundation for Research and Innovation (HFRI) and the General Secretariat for Research and Technology (GSRT), under grant agreement no. 27361/21-02-2019.

References

[1] E. Peiner, Anodic dissolution during electrochemical carrier-concentration profiling of silicon, J. Electrochem. Soc. 139 (1992) 552, https://doi.org/10.1149/1.2069255.
[2] B. Sermage, Z. Essa, N. Taleb, M. Quillec, J. Aubin, J.M. Hartmann, M. Veillerot, Electrochemical capacitance voltage measurements in highly doped silicon and silicon-germanium alloys, J. Appl. Phys. 119 (2016), https://doi.org/10.1063/1.4946890.
[3] G.E. Yakovlev, D.S. Frolov, A.V. Zubkova, E.E. Levina, V.I. Zubkov, A. V. Solomonov, O.K. Sterlyadkin, S.A. Sorokin, Investigation of ion-implanted photosensitive silicon structures by electrochemical capacitance–voltage profiling, Semiconductors. 50 (2016) 320–325, https://doi.org/10.1134/S1063782616030234.
[4] D.S. Frolov, G.E. Yakovlev, V.I. Zubkov, Technique for the electrochemical capacitance–voltage profiling of heavily doped structures with a sharp doping profile, Semiconductors. 53 (2019) 268–272, https://doi.org/10.1134/s1063782619020076.
[5] N. Sieber, H.E. Wulf, D. Röser, P. Kurps, Application of electrochemical capacitance - voltage measurements for profiling in silicon, Phys. Status Solidi 126 (1991) K123–K127, https://doi.org/10.1002/pssa.2211260234.
[6] A. Gharbi, B. Remaki, A. Halimaoui, D. Bensahel, A. Souifi, P-type silicon doping profiling using electrochemical anodization, J. Appl. Phys. 109 (2011), https://doi.org/10.1063/1.3534005.
[7] A. Gharbi, B. Remaki, A. Halimaoui, D. Bensahel, A. Souifi, Investigation of current-voltage characteristics of p-type silicon during electrochemical anodization and application to doping profiling, Phys. Status Solidi Curr. Top. Solid State Phys. 8 (2011) 784–787, https://doi.org/10.1002/pssc.201000343.
[8] M. Ligeon, F. Muller, R. Herino, F. Gaspard, A. Halimaoui, G. Bomchil, Application of porous silicon formation selectivity to impurity profiling in p-type silicon substrates, J. Appl. Phys. 66 (1989) 3814–3819, https://doi.org/10.1063/1.344044.
[9] L. Canham, Properties of Porous Si, INSPEC, London, UK, 1997.
[10] D. Macdonald, L.J. Geerligs, Recombination activity of interstitial iron and other transition metal point defects in p- and n-type crystalline silicon, Appl. Phys. Lett. 85 (2004) 4061–4063, https://doi.org/10.1063/1.1812833.
[11] J. Schmidt, R. Krain, K. Bothe, G. Pensl, S. Beljakowa, Recombination activity of interstitial chromium and chromium-boron pairs in silicon, J. Appl. Phys. 102 (2007), https://doi.org/10.1063/1.2822452.
[12] I. Leontis, M.A. Botzakaki, S.N. Georga, A.G. Nassiopoulou, Study of Si nanowires produced by metal-assisted chemical etching as a light-trapping material in n-type c-Si solar cells, ACS Omega. 3 (2018) 10898–10906, https://doi.org/10.1021/acsomega.8b01049.
[13] F. Kiefer, J. Krugener, F. Heinemeyer, H.J. Osten, R. Brendel, R. Peibst, Structural investigation of printed Ag/Al contacts on silicon and numerical modeling of their contact recombination, IEEE J. Photovoltaics. 6 (2016) 1175–1182, https://doi.org/10.1109/JPHOTOV.2016.2591318.
[14] P. Rothhardt, S. Meier, R. Hoenig, A. Wolf, D. Biro, Influence of surface near doping concentration on contact formation of silver thick film contacts, Sol. Energy Mater. Sol. Cells 153 (2016) 25–30, https://doi.org/10.1016/j.solmat.2016.03.030.
[15] G. Ayvazyan, A. Vardanyan, G. Makaryan, Method of Determination of Silicon P-N Junction Depth, WO 02/03448 A1, 2002.
[16] S.B. Felch, R. Brennan, S.F. Corcoran, G. Webster, A comparison of three techniques for profiling ultra-shallow p+−n junctions, Nucl. Inst. Methods Phys. Res. B 74 (1993) 156–159, https://doi.org/10.1016/0168-583X(93)95035-4.
[17] D.K. Schroder, Semiconductor Material and Device Characterization, 2nd ed., Wiley, New York, 1998.
[18] S.M. Sze, Physics of Semiconductor Devices, 3rd ed., Wiley, Hoboken, New Jersey, 2007.